CHAPTER V

INVESTIGATION OF EFFECT OF REACTOR STRUCTURE

Evidently the electron attachment method has already shown great potential for commercial application in gas purification. The next logical question is how to optimize or scale up the device. As a first step the effect of the reactor structure on the removal efficiency must be understood. Any structural change is expected to affect simultaneously several important factors such as discharge current, electron energy, electric field strength, migratory distance, and residence time in the reactor. Thus, this chapter describes the effects of the reactor structure on the resulting removal efficiency with respect to each of three dilute gaseous pollutants: methyl iodide (CH_3I), 1,1,2-trichloro-1,2,2-trifluoroethane ($C_2Cl_3F_3$) and acetaldehyde (CH_3CHO). Their removal efficiencies have been calculated by using Eq. (4.1). The experimental conditions of each inlet gas are shown in **Table 5.1**.

Table 5.1 Experimental conditions of inlet gas

Sample gas	Concentration [ppm]	Total flow rate [m^3s^{-1}]	Space velocity [h^{-1}]
CH_3I	80	4.08×10^{-6}	46.3
$C_2Cl_3F_3$	400	1.67×10^{-6}	18.9
CH_3CHO	100	5.00×10^{-6}	56.7

A material packed in a GC column, used for detecting the concentrations of each gas was polydivinylbenzene (Millopore Corp., Porapak Q) with 80~100 mesh. The experimental conditions of a gas chromatograph with a flame ionization detector (FID), corresponding to each gas were given in **Table 5.2**.

Table 5.2 Experimental conditions of FID gas chromatograph

Sample gas	Column temperature (°c)	Injection temperature (°c)	Detector temperature (°c)	Retention time (min)
CH_3I	150	200	220	7.0
$C_2Cl_3F_3$	180	250	250	5.4
CH_3CHO	120	150	150	4.1

In this chapter, the effects of the reactor structure, namely, the cathode diameter, the anode (reactor) shape, and the number of cathodes on the removal efficiency with respect to the above gases were investigated.

5.1 Cathode diameter

5.1.1 Experimental

The experiments can be categorized into two parts: 1) removal from dry air (20% O_2), and 2) removal from dry N_2. A variety of cathode diameters,

0.05, 0.1, 0.2, 0.3, 0.5, 0.8, 1.0, 1.26, and 1.6 mm, was used. The diameter and length of the anode were 38 mm and 280 mm, respectively.

5.1.2 Results and Discussion

As mentioned earlier, the probability of electron attachment depends on electron energy, and type of gas component. Electron energy in the reactor depends on the ratio of the electric field strength, E, to the total gas pressure, p, i.e. E/p. Electrons are accelerated in E, and collisions between electrons and gas molecules cause deceleration in p. Thus, if E/p is high, electron energy is also high. The electric field strength E is as follows.

$$E = V/\{r \ln (R/R_0)\} \tag{5.1}$$

As seen in Eq. (5.1), electric field strength increases when the corona voltage increases. **Figure 5.1** shows the relation between the discharge current, I, and voltage, V, for CH_3I removal from dry air. Obviously, a thicker cathode diameter requires a significantly higher V to yield the same current. Similar tendency to the case of CH_3I removal from air also happened to CH_3I removal from N_2 as well as $C_2Cl_3F_3$ and CH_3CHO removal (see **Appendix E**). According to Eq. (5.1), an increase in the cathode diameter contributes to an increase in E under a constant V. It can be said that the thicker the cathode diameter, the higher the electric field strength, E.

The average electric field strength per pressure is given as follows.

$$< E/p > = \frac{\int_{R_0}^{R} (2\pi r)(E/p)\,dr}{\pi(R^2 - R_0^2)} = \frac{2V}{p(R+R_0)\ln(R/R_0)} \tag{5.2}$$

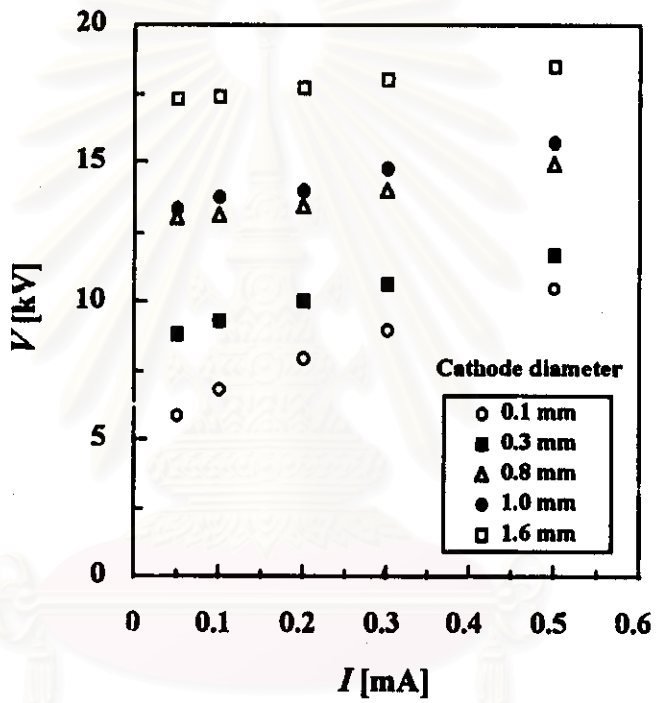

Figure 5.1 Discharge current-voltage relationship for CH_3I removal from air (20% O_2); (anode diameter x length = 38 mm x 280 mm, C_{in} = 80 ppm, SV = 46.3 h^{-1})

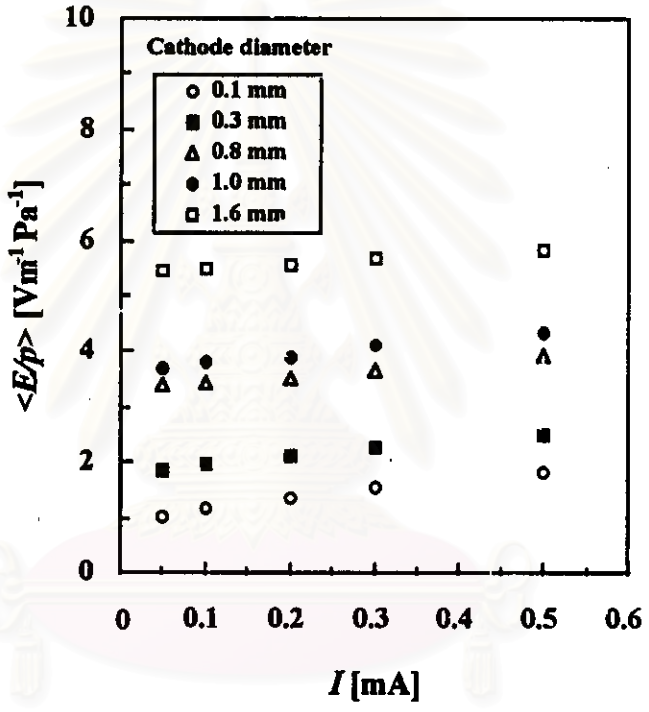

Figure 5.2 Average electric field strength/pressure as a function of discharge current for CH_3I removal from air (20% O_2); (anode diameter x length = 38 mm x 280 mm, C_{in} = 80 ppm, SV = 46.3 h^{-1})

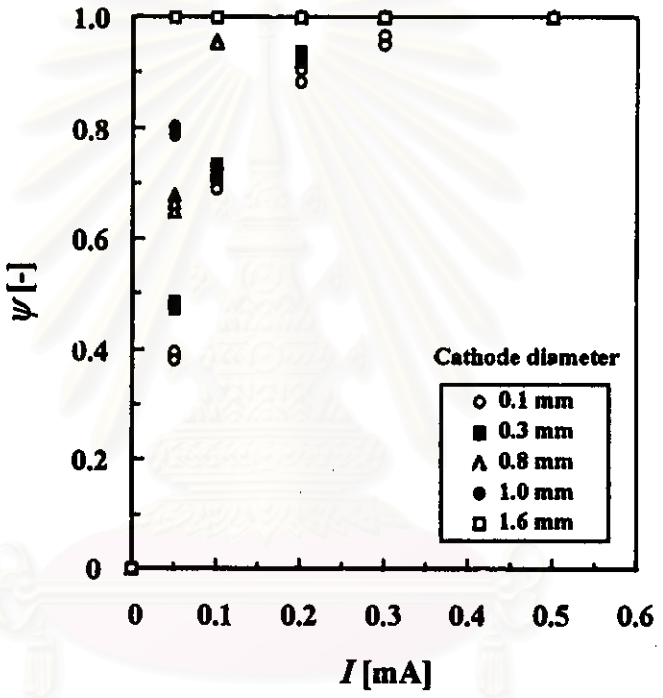

Figure 5.3 Removal efficiency of CH_3I from air (20% O_2) as a function of discharge current; (anode diameter x length = 38 mm x 280 mm, C_{in} = 80 ppm, SV = 46.3 h^{-1})

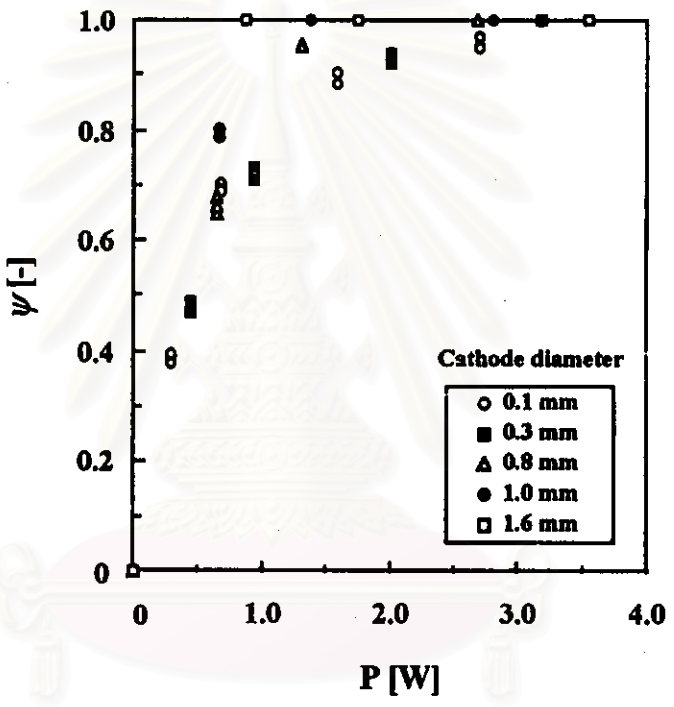

Figure 5.4 Removal efficiency of CH_3I from air (20% O_2) as a function of electric power; (anode diameter x length = 38 mm x 280 mm, C_{in} = 80 ppm, SV = 46.3 h^{-1})

Figure 5.2 shows $\langle E/p \rangle$ for CH_3I removal from air as a function of I. It is obvious that $\langle E/p \rangle$ increases as the cathode diameter increases, or in order words, electron energy increases with increasing cathode diameter.

Figure 5.3 shows the observed removal efficiency, ψ, of CH_3I from air corresponding to the different sizes of the cathode. It is found that a thicker cathode provides a higher ψ. Similar removal behaviors for other sample gases are also observed (see **Appendix E**).

Although a thicker cathode wire provides a higher ψ, the required voltage, V, becomes higher as well, resulting in a higher power consumption. **Figure 5.4** depicts ψ for CH_3I removal from air as a function of electric power, P. It conclusively shows that a thicker cathode provides a higher ψ when comparison is made at the same P. Similar tendency was observed in the cases of $C_2Cl_3F_3$ and CH_3CHO (see **Appendix E**).

5.2 Anode dimensions

5.2.1 Experimental

Three different shapes for the equivolume cylindrical reactor vessel, as shown in **Figure 5.5**, whose diameter (mm) and length (mm) are 76 x 70, (largest diameter), 38 x 280 (intermediate diameter), and 19 x 1,120 mm (smallest diameter), were used. The cathode diameters used for the individual removal of CH_3I, $C_2Cl_3F_3$, and CH_3CHO were 0.3, 0.3, and 0.2 mm, respectively.

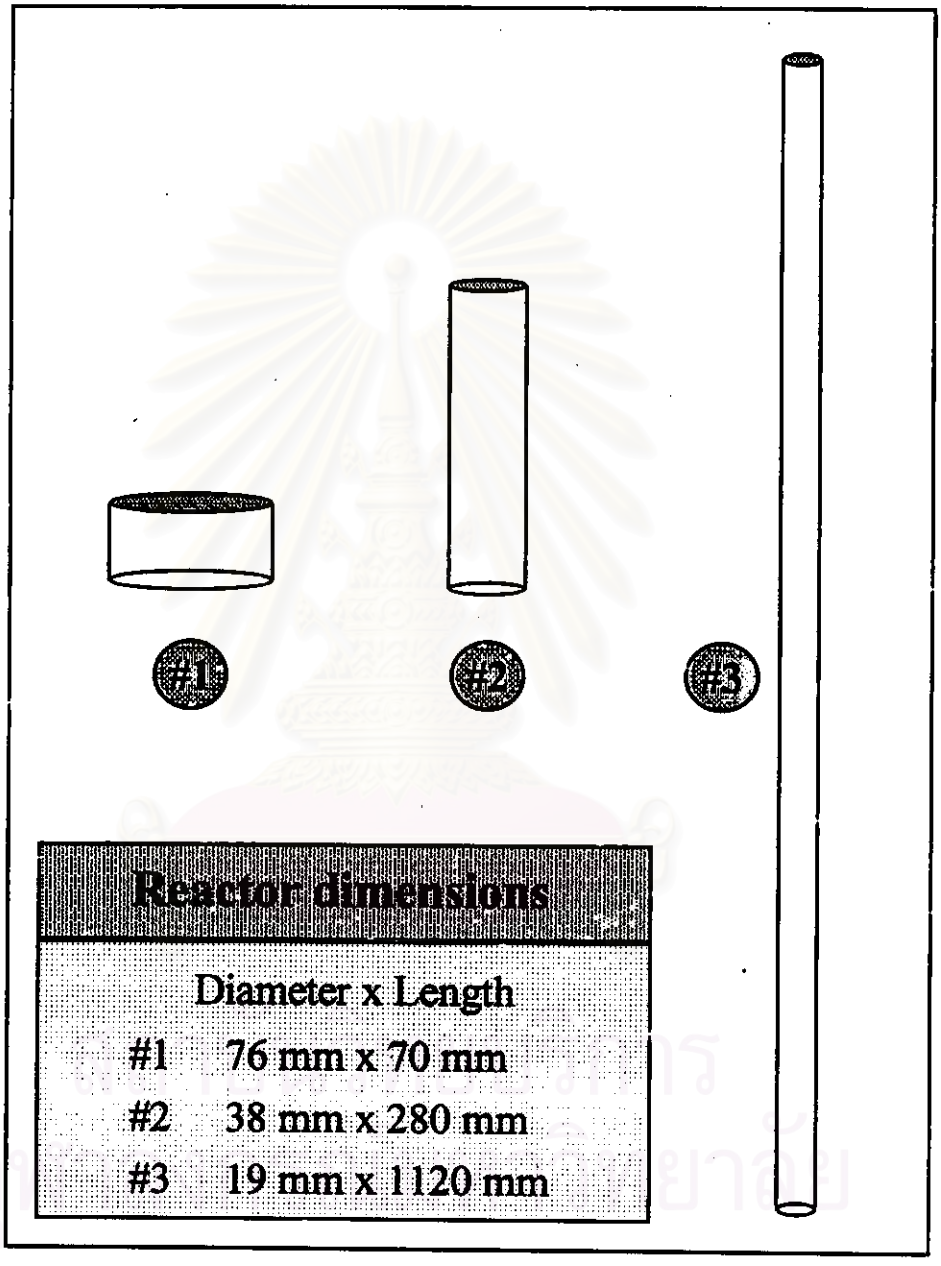

Figure 5.5 Three different anode shapes of reactor

5.2.2 Results and Discussion

Figure 5.6 compares the removal efficiency of $C_2Cl_3F_3$ from air among three anode (reactor) shapes. The order of efficiency is: smallest reactor diameter > intermediate diameter > largest diameter. **Figure 5.7** shows the relations between ψ and P. It conclusively shows that the smaller the anode diameter, the higher the removal efficiency. Similar tendency was observed for the other two cases (see **Appendix F**).

The applied voltage and $\langle E/p \rangle$ for $C_2Cl_3F_3$ removal from air are shown in **Figures 5.8 and 5.9**. As seen in **Figure 5.8**, the larger the reactor diameter, the higher the required V. However, **Figure 5.9** shows a different order of E/p vs. I from that of V vs. I in **Figure 5.8**. According to the typical electric field profile, this comparison suggests that the average electron energy in the smallest reactor diameter is largest, while the other two shapes have approximately the same electron energy. Similar tendency was observed for the other cases (see **Appendix F**).

From the previous discussion in **Section 5.1**, it is found that ψ is enhanced as electron energy becomes higher. Since the orders of ψ vs. I and $\langle E/p \rangle$ vs. I differ as the anode shape changes, the difference in removal efficiency can not be attributed solely to the electron energy. Since all three volumes are equal, the mean residence times in the three reactors are the same. However, the larger the reactor diameter, the longer the average distance a negatively charged molecule would need to migrate to reach the anode. When the average electron energy is about equal, a smaller fraction of the charged molecules in the larger-diameter reactor would be able to reach the anode within the available residence time. This is the reason that the 76 mm-diameter

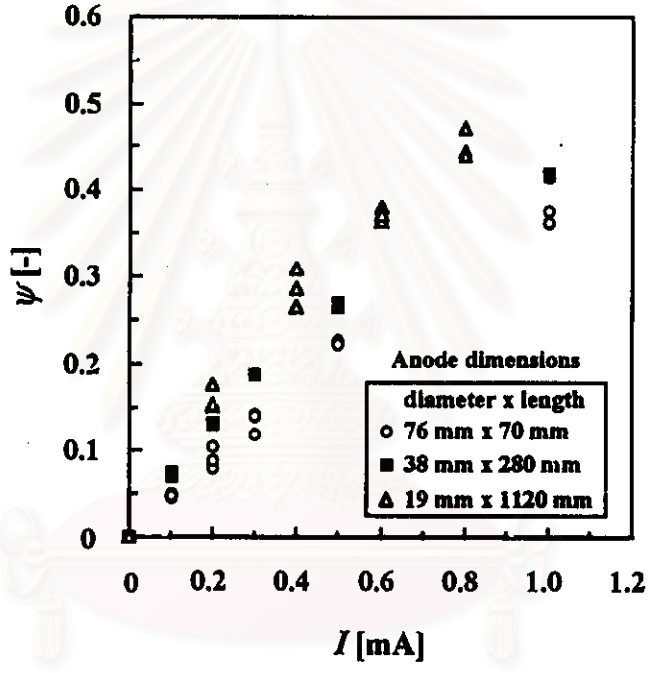

Figure 5.6 Removal efficiency of $C_2Cl_3F_3$ from air (20% O_2) as a function of discharge current; (cathode diameter = 0.3 mm, C_{in} = 400 ppm, SV = 18.9 h^{-1})

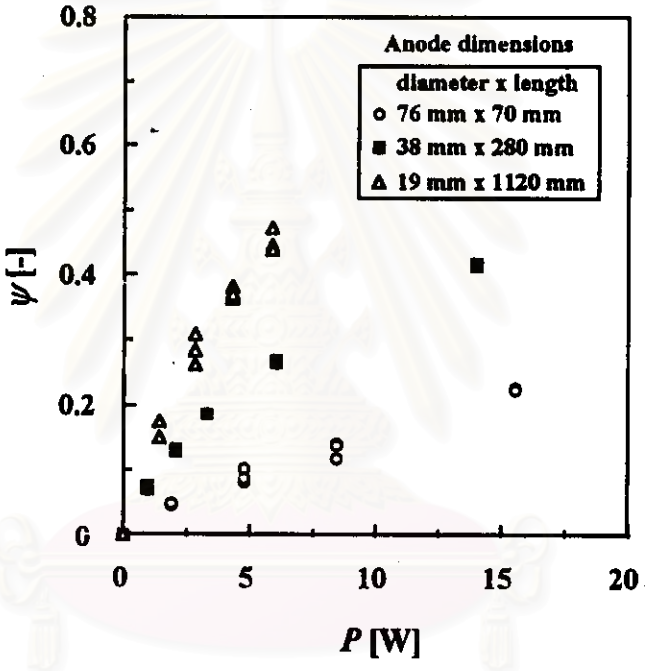

Figure 5.7 Removal efficiency of $C_2Cl_3F_3$ from air (20% O_2) as a function of electric power; (cathode diameter = 0.3 mm, C_{in} = 400 ppm, SV = 18.9 h^{-1})

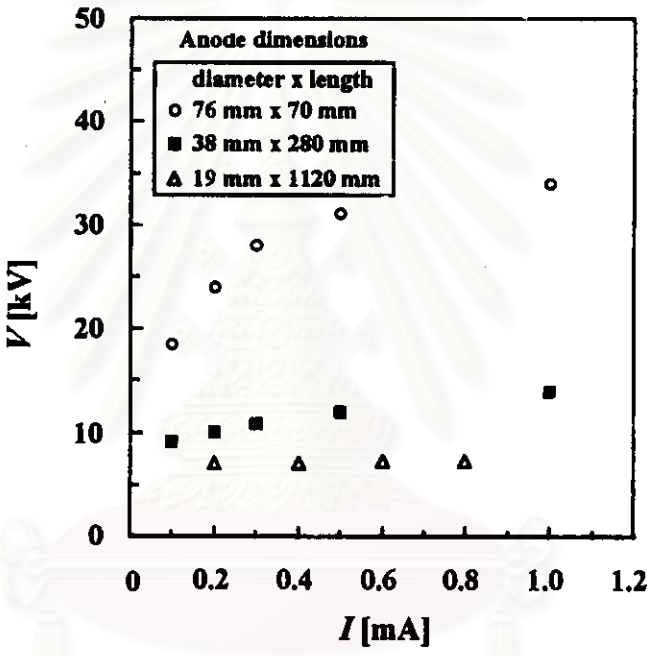

Figure 5.8 Discharge current-voltage relationship for $C_2Cl_3F_3$ removal from air (20% O_2); (cathode diameter = 0.3 mm, C_{in} = 400 ppm, SV = 18.9 h^{-1})

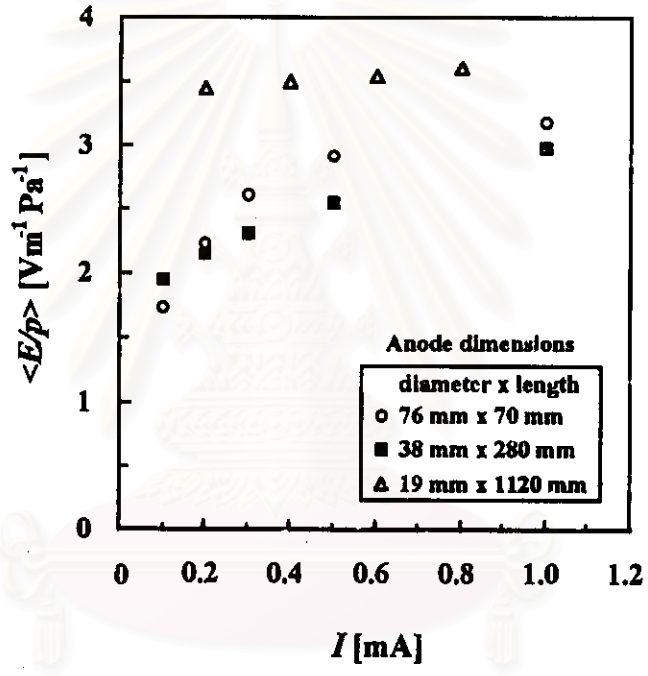

Figure 5.9 Average electric field strength/pressure as a function of discharge current for $C_2Cl_3F_3$ removal from air (20% O_2); (cathode diameter = 0.3 mm, C_{in} = 400 ppm, SV = 18.9 h^{-1})

reactor has about half the removal efficiency of the 38 mm-diameter one though their average *E/p* values are nearly equal.

One important conclusion is that to enhance the removal efficiency, the reactor should be as long and slender as technically feasible, provided the resulting higher velocity does not cause excessive pressure drop and turbulence. Efficiency enhancement could be obtained even when *P*, i.e. power consumption, is lowered significantly to achieve comparable average electron energy.

5.3 Single vs. multiple cathodes

5.3.1 Experimental

The cross section of the two reactor types are illustrated in **Figure 5.10**. Both have the same design features except for the number of cathode wires, one vs. five. The diameter and length of the anode were 38 mm and 280 mm, respectively. The cathode diameter used for each gas was 0.3 mm.

5.3.2 Results and discussion

Figures 5.11 and 5.12 compare the effect of the cathode number on ψ for removal of CH_3CHO from air in terms of *I* and *P*, respectively. Using either criterion, the single-cathode reactor clearly exhibits higher removal efficiency than the 5-cathode one.

It was visually confirmed that, when high voltage was applied to the 5-cathode reactor, the corona of the central cathode failed to appear. This means that some "dead space" (corona-free space) existed around the central

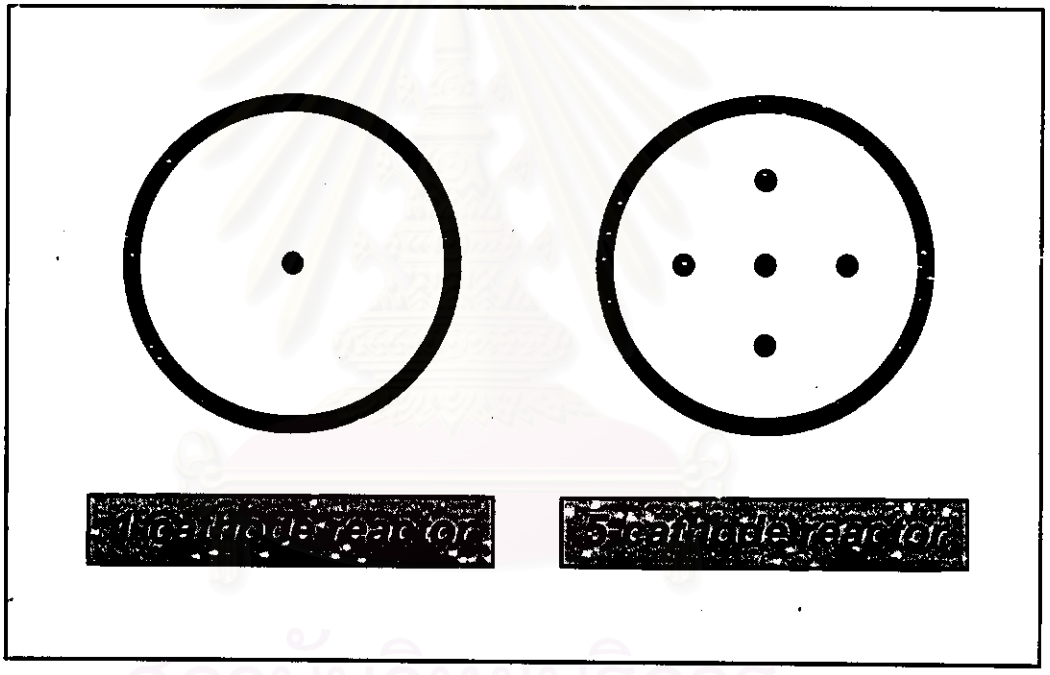

Figure 5.10 Cross sections of two types of reactor

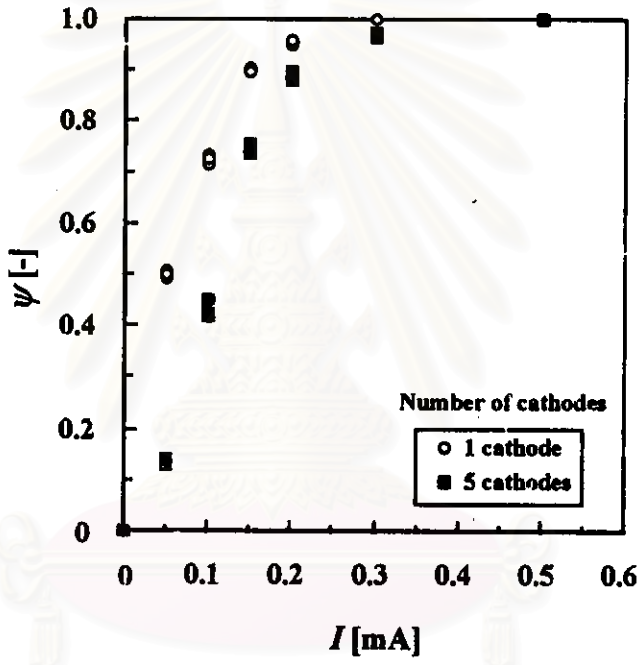

Figure 5.11 Removal efficiency of CH_3CHO from air (20% O_2) as a function of discharge current; (cathode diameter = 0.3 mm, anode diameter x length = 38 mm x 280 mm, C_{in} = 100 ppm, SV = 56.7 h^{-1})

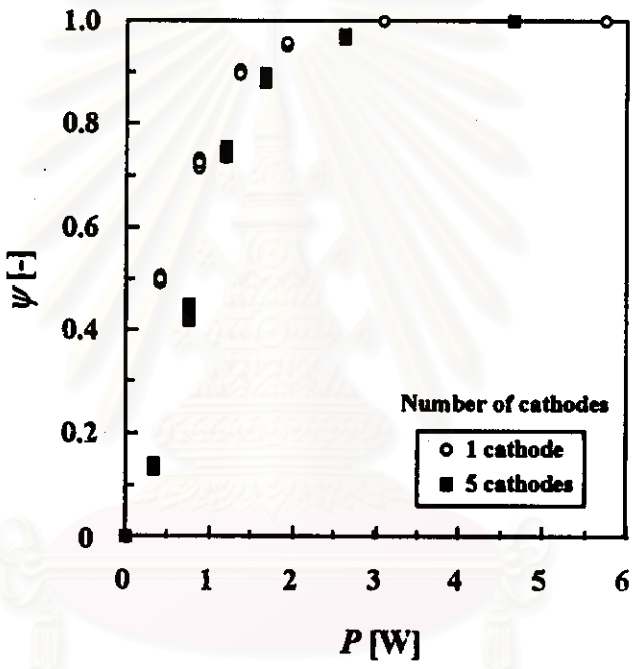

Figure 5.12 Removal efficiency of CH_3CHO from air (20% O_2) as a function of electric power; (cathode diameter = 0.3 mm, anode diameter x length = 38 mm x 280 mm, C_{in} = 100 ppm, SV = 56.7 h^{-1})

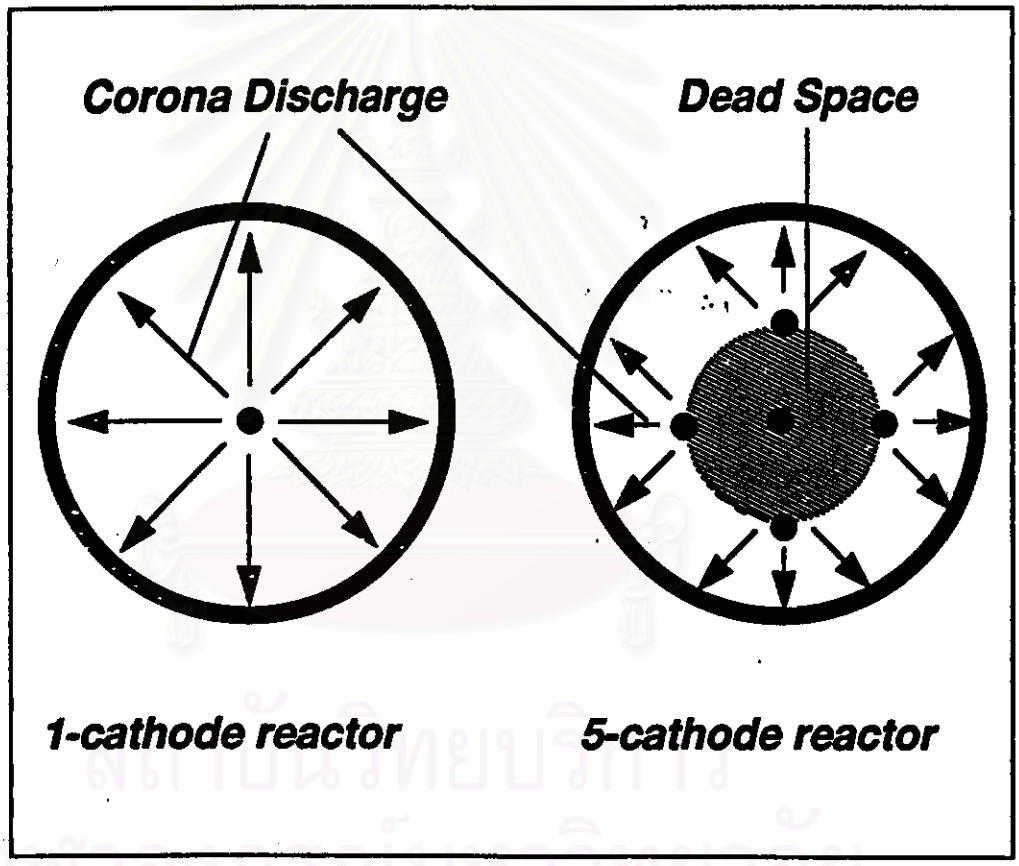

Figure 5.13 Distribution of density of electrons in reactors

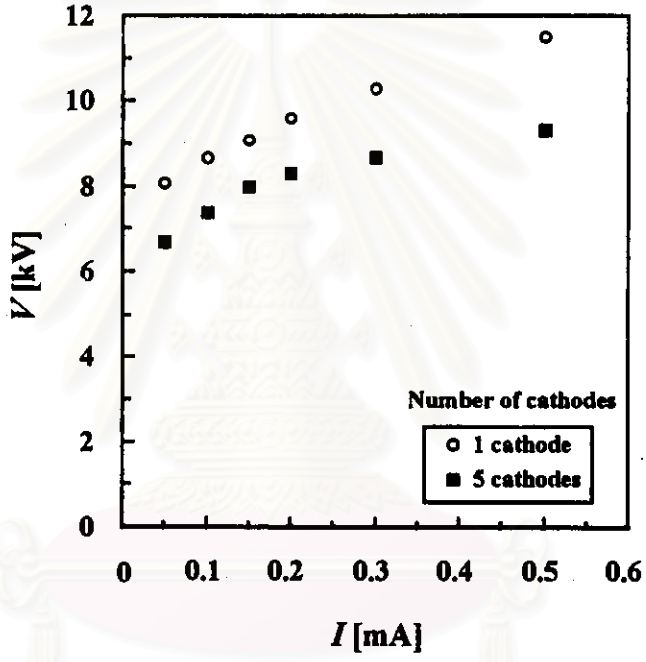

Figure 5.14 Discharge current-voltage relationship for CH_3CHO removal from air (20% O_2); (cathode diameter = 0.3 mm, anode diameter x length = 38 mm x 280 mm, C_{in} = 100 ppm, SV = 56.7 h^{-1})

cathode wire. **Figure 5.13** depicts the distribution of density of electrons in the reactors. This results in a lower required V compared to the single-cathode reactor, as can be seen in **Figure 5.14**, because of the shorter distance between the anode and the other four cathodes. Conclusively, the dead space causes a lower ψ in the 5-cathode reactor. Similar removal results for CH_3I and $C_2Cl_3F_3$ are observed (see **Appendix G**).

5.4 Conclusion

The structural effects of the corona-discharge reactor on individual removal efficiency of CH_3I, $C_2Cl_3F_3$ and CH_3CHO have been investigated experimentally. The experimental results reveal that the thicker the cathode, the higher the removal efficiency, provided the discharge voltage remains stable. Regarding the anode dimensions of equivolume reactors, it has been found that the smaller the reactor diameter, the higher the removal efficiency despite lower energy consumption. As for the number of cathodes, the single-cathode reactor definitely exhibits higher removal efficiency than the multiple-cathode one.

Table 5.3 summarizes the maximum removal efficiency observed in the present study corresponding to the individual removal of each pollutant mixed with N_2 or air. Although most cases in **Table 5.3** indicate the incomplete removal efficiency, it can be expected that their removal efficiencies would be enhanced by increasing the discharge current for each case above the range of the discharge current investigated in the present work. However, the experimental results reveal that the applied voltage increases with increasing discharge current. The discharge current increase is, therefore, limited by the maximum allowable voltage or, in other words, by the capability of the high-voltage DC generator.

Table 5.3 Maximum removal efficiency observed in this study

Sample gas	C_{in} [ppm]	SV [h^{-1}]	I [mA]	V [kV]	P [W]	ψ_{max} (%)
CH_3I in N_2	80.3	46.3	1.5	10.9	16.35	**76.7**
CH_3I in air	80.3	46.3	0.05	17.3	0.87	**100***
$C_2Cl_3F_3$ in N_2	398.4	18.9	1.0	17.5	17.5	**94.4**
$C_2Cl_3F_3$ in air	398.4	18.9	1.0	17.3	17.3	**49.2**
CH_3CHO in N_2	99.6	56.7	1.5	4.0	6.00	**39.3**
CH_3CHO in air	99.6	56.7	0.2	11.3	2.26	**100***

* C_{out} is lower than the detection limit (0.1 ppm).

Furthermore, it is found that CH_3I and CH_3CHO removal from N_2 shows worse removal efficiency than that from dry air (20% O_2). On the other hand, $C_2Cl_3F_3$ removal from N_2 shows better removal efficiency than that from air. These results suggest that the presence of O_2 in a gas mixture may positively or negatively affect the removal efficiency of the targeted gaseous pollutant. This agrees with the results obtained by Tamon et al. (1996) that the presence of some common coexisting gaseous components such as O_2 and H_2O vapor is likely to enhance or, conversely, retard the removal efficiency of gaseous pollutants. Since the present research emphasizes the structural effects of the corona-discharge reactor on the removal efficiency, a study regarding the role of coexisting O_2 on the removal efficiency is beyond the scope of the present study.